

Chiral transfer of angular momentum

By H. K. Moffatt¹ and V. A. Vladimirov^{2,3,4}

¹Department of Applied Mathematics and Theoretical Physics,
Wilberforce Road, Cambridge CB3 0WA, UK

²Sultan Qaboos University, Oman, ³University of York, UK, ⁴University of Leeds, UK

(Received 16 April 2019)

Suppose that viscous fluid is contained in the space between a fixed sphere S_2 and an interior sphere S_1 which moves with time-periodic velocity $\mathbf{U}(t)$ and angular velocity $\boldsymbol{\Omega}(t)$, with $\langle \mathbf{U}(t) \rangle = \langle \boldsymbol{\Omega}(t) \rangle = 0$. It is shown that, provided this motion is chiral in character, it can drive a flow that exerts a non-zero torque on S_2 . Thus angular momentum can be transferred through this mechanism.

1. Introduction

Consider the following simple problem: suppose that a sphere S_1 of radius r_1 is contained inside a fixed sphere S_2 of radius $r_2 > r_1$, the space between being filled with viscous fluid. Suppose that S_1 is moved with a time-periodic velocity $\mathbf{U}(t)$ and angular velocity $\boldsymbol{\Omega}(t)$ with zero time average: $\langle \mathbf{U}(t) \rangle = \langle \boldsymbol{\Omega}(t) \rangle = 0$, as in the sketch of Figure 1(a). Is it possible that such a motion can generate a mean torque on the fixed sphere S_2 ? We shall show by explicit example that the answer is positive, the effect arising only if the flow between the spheres has the property of chirality (lack of reflection symmetry); in this respect it is analogous to the helicity effect that is responsible for the self-excitation of magnetic field in a conducting fluid (Moffatt 1978).

2. A simple planar model

Suppose first that fluid of viscosity μ and kinematic viscosity $\nu = \mu/\rho$ fills the space $|z| < 1$ between two rigid plane boundaries $z = \pm 1$, and that a circular disc of radius $a \gg 1$ and negligible thickness is immersed in the fluid parallel to the boundaries at position $z = d_0$ with $|d_0| < 1$. We adopt cylindrical polar coordinates (r, φ, z) , where r is the radial distance from the axis of the disc. The situation is sketched in Figure 1(b). Suppose now that the disc is caused to oscillate vertically so that its position at time t is $d(\tau) = d_0 + \zeta(\tau)$, where $\tau \equiv \sigma t$ and σ is a frequency. The disc is simultaneously caused to rotate about its axis with angular velocity $\omega(\tau)$. Both functions $\zeta(\tau)$ and $\omega(\tau)$ are assumed to be 2π -periodic with zero average, $\langle \zeta(\tau) \rangle = \langle \omega(\tau) \rangle = 0$.

Let U_0 be the maximum speed of the disc during its periodic motion. We assume that the Reynolds number $\text{Re} = U_0 a / \nu$ and the Stokes number $\text{St} = \sigma a^2 / \nu$ are small, so that inertia effects in the fluid may be neglected; the methods of ‘thin-film’ lubrication theory (e.g. Batchelor 1967) are then applicable. In these circumstances, the poloidal (r, z) and toroidal (φ) components of the equations of motion are decoupled. We need here consider only the toroidal component of velocity $v(r, z, \tau)$ within the gaps $-1 < z < d$ and $d < z < 1$. This is essentially a ‘Couette-flow’ situation in both gaps, with boundary conditions $v = 0$ at $z = \pm 1$ and $v = \omega r$ at $z = d \pm 0$. A simple calculation of the total

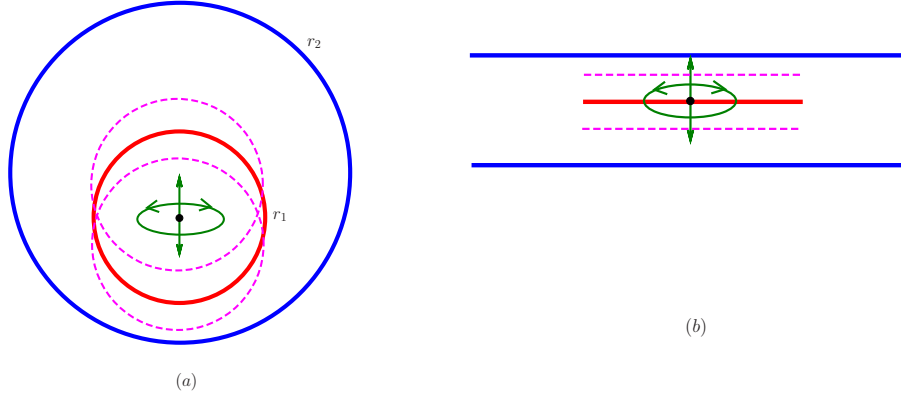


Figure 1: (a) Two-sphere configuration; the outer sphere is fixed and the inner sphere oscillates between the (dashed) limits indicated, and rotates about the axis of symmetry with time-periodic angular velocity $\omega(t)$ with $\langle \omega(t) \rangle = 0$. (b) Corresponding oscillating-disc model.

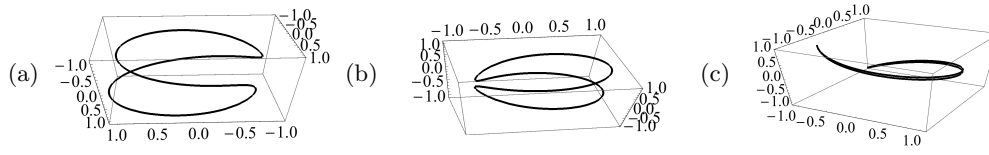


Figure 2: Trajectories of a point on the disc with velocity (2.3); $r_0 = 1$, $d_0 = 0.2$, $\lambda = 0.76$, $\omega_0 = 2.5$; (a) $\phi_0 = 0$, (b) $\phi_0 = \pi/4$, (c) $\phi_0 = \pi/2 - 0.05$.

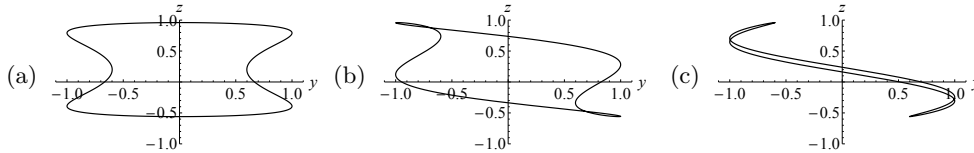


Figure 3: Projections on the plane $x = 0$ of the trajectories of Figure 2.

instantaneous torque $G(\tau)$ exerted on the plates yields

$$G(\tau) = \kappa \omega D \quad \text{where} \quad D \equiv \frac{1}{2} \left(\frac{1}{1-d} + \frac{1}{1+d} \right) = \frac{1}{1-d^2} \quad \text{and} \quad \kappa \equiv \pi \mu a^4. \quad (2.1)$$

Hence the average torque on the plates over a period of the disc motion is

$$\langle G(\tau) \rangle = \kappa \chi \quad \text{where} \quad \chi \equiv \langle \omega(\tau) D(\tau) \rangle. \quad (2.2)$$

(There is an equal and opposite mean torque exerted by the fluid on the moving disc.)

By way of example, let

$$d(\tau) = d_0 + \zeta(\tau), \quad \zeta(\tau) = \zeta_0 \cos \tau, \quad \omega(\tau) = \omega_0 \cos(\tau + \phi_0), \quad (2.3)$$

where $|d_0 \pm \zeta_0| < 1$ and where $\omega_0, \phi_0, d_0, \zeta_0$ are non-negative constants. The trajectory of any point of the disc then has parametric equation $r = r_0$, $\varphi = \varphi_0 + \int_0^\tau \omega(\tau') d\tau'$, $z = d(\tau)$, and, being periodic in τ with period 2π , is a closed curve on the cylinder $r = r_0$. Three examples of such trajectories, with $r_0 = 1$, $d_0 = 0.2$, $\zeta_0 = 0.76$, $\omega_0 = 2.5$, and phase differences $\phi_0 = 0, \pi/4$ and $\pi/2 - 0.05$, are shown in Figure 2. These trajectories wind

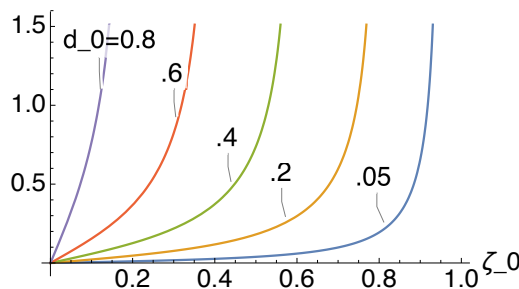


Figure 4: The functions $g(d_0, \zeta_0)$ defined by (2.5) for five values of d_0 and for $0 < \zeta_0 < 1 - d_0$ in each case.

almost once round the cylinder $r = r_0$, then reverse and wind back so that the closed curve makes zero net turns round the cylinder, as most clearly seen in Figure 2(c). For the limiting case $\phi_0 = \pi/2$, the trajectory is a portion of a helix traversed up and down periodically. Figure 3 shows projections of the same three figures on the plane $x = 0$; note that this projection encloses a finite area (with positive or negative contributions from regions whose boundaries are traversed in an anticlockwise or clockwise sense) which decreases (actually proportional to $\cos \phi_0$) as ϕ_0 increases from 0 to $\pi/2$.

Evaluation of the mean $\langle G \rangle$ from (2.3) now yields:

$$\langle G \rangle = \kappa \omega_0 g(d_0, \zeta_0) \cos \phi_0, \quad (2.4)$$

where

$$g(d_0, \zeta_0) \equiv \frac{1}{2\zeta_0} \left[\frac{1 - d_0}{\sqrt{(1 - d_0)^2 - \zeta_0^2}} - \frac{1 + d_0}{\sqrt{(1 + d_0)^2 - \zeta_0^2}} \right]. \quad (2.5)$$

The functions $g(d_0, \zeta_0)$ are shown in Figure 4 for $d_0 = 0.2, 0.4, 0.6, 0.8$ and the relevant range in each case, $0 < \zeta_0 < 1 - d_0$. Note the singular behaviour as $\zeta_0 \rightarrow 1 - d_0$; this simply reflects the torque singularity that is to be expected when the gap between the disc and the boundary $z = 1$ tends to zero.

It is easy to understand the physical origin of this mean torque. Consider just the time interval $-\pi < \tau < \pi$. If $d_0 > 0$ and $\zeta_0 > 0$, then the disc is at its shortest distance from the upper fixed boundary when $\tau = 0$; if $\phi_0 = 0$, the instantaneous torque on this boundary is then maximal and in the positive direction (i.e. the direction of increasing φ); when $\tau = \pi$, the disc is at its furthest distance from the upper boundary (as most evident in Figure 3(a)) and the instantaneous torque is then minimal and in the negative direction. Hence, the averaged torque on the upper boundary is positive. At the same time, a similar consideration for the more remote lower boundary results in a smaller average torque in the negative direction. The time-averaged total torque is therefore positive when $\phi_0 = 0$, as confirmed by (2.4) and (2.5) and Figure 4. Note the $\cos \phi_0$ dependence on the phase factor in (2.5), the mean effect being maximal when $\phi_0 = 0$, i.e. when $D(\tau)$ and $\omega(\tau)$ are in phase.

If $\phi_0 = \pi/2$ the disc motion is reversed from one half-period to the next. By the reversibility theorem for Stokes flow, the fluid flow is similarly reversed, and the contributions to the mean torque are therefore equal and opposite in the two half-periods. This explains why a mean torque is generated only if $\phi_0 \neq \pi/2$.

When $d_0 = 0$ in (2.3), then in (2.4) $\langle G \rangle = 0$ also, i.e. the total averaged torque generated on both boundaries taken together is zero, as might be expected from symmetry.

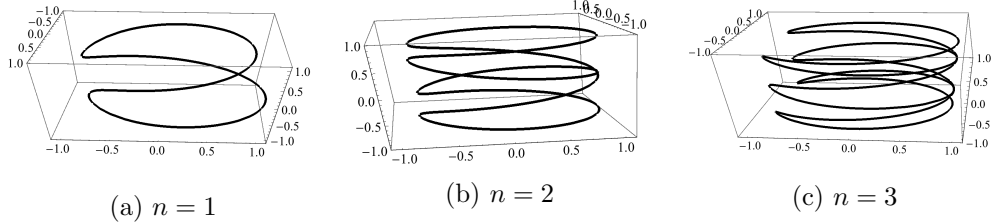


Figure 5: Trajectories of a point on the disc with velocity (2.6) for different n ; $d_0 = 0$, $\zeta_0 = .8$, $\omega_0 = 2.5$.

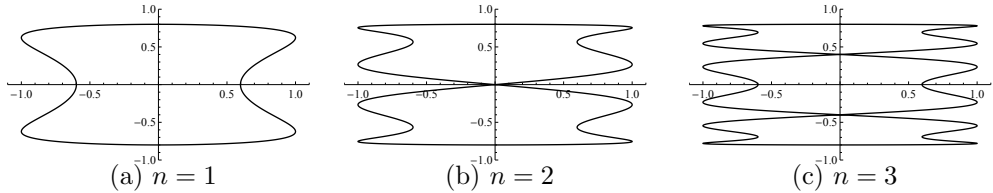


Figure 6: Projections on the plane $x = 0$ of the trajectories of Figure 5.

The above physical description suggests however how torque may be generated through modification of $\omega(\tau)$. Thus suppose for example that

$$\omega(\tau) = \omega_0 \cos n\tau, \quad d(\tau) = \zeta_0 \cos \tau, \quad (2.6)$$

where n is a positive integer. Figure 5 shows three possibilities for the trajectories of a point on the disc, and Figure 6 shows corresponding projections with $\omega(t)/\omega_0 = \cos \tau$, $2 \cos 2\tau$, and $3 \cos 3\tau$ (so $\varphi(\tau)/\omega_0 = \sin \tau$, $\sin 2\tau$, $\sin 3\tau$ respectively). For $n = 1$ or 3 (and more generally for any odd n) such a trajectory has the opposite sense (clockwise/anticlockwise) near the boundaries $z = \pm 1$, whereas for $n = 2$ (and more generally for any even n) it has the same sense near both boundaries. We may then expect that $\langle G \rangle$ should be nonzero only if n is even.

This is confirmed by evaluation of (2.2) for the motion (2.6), which yields (with the help of Gradshteyn & Ryzhik 2007, p.391, formula 3.613)

$$\langle G(\zeta_0, n) \rangle = \kappa \omega_0 g(\zeta_0, n), \quad (2.7)$$

where

$$g(\zeta_0, n) = \frac{1 + (-1)^n}{2\sqrt{1 - \zeta_0^2}} \left(\frac{1 - \sqrt{1 - \zeta_0^2}}{\zeta_0} \right)^n. \quad (2.8)$$

For n even, $g(\zeta_0, n) \sim (\zeta_0/2)^n$ for small ζ_0 ; the first three ($n = 2, 4, 6$) are plotted in Figure 7. Note again the (expected) singular behaviour as $\zeta_0 \rightarrow 1$, when the disc makes instantaneous contact with each boundary $z = \pm 1$ once in each period of the motion.

The quantity $\chi = \langle \omega(\tau)D(\tau) \rangle$ that appears in the above examples is a pseudo-scalar, which can be non-zero only if the motion of the disc is chiral in character (i.e. lacking reflection symmetry). It is in this respect that the phenomenon of mean-torque generation is analogous to the phenomenon of spontaneous dynamo-generation of magnetic field in a conducting fluid, resulting from non-zero mean helicity of a random wave field. In that context, a phase shift between velocity and magnetic perturbations is required to provide a nonzero α -effect (Moffatt 1978, §7.7). Similarly, in the present context, there must be a phase shift between the vertical displacement $d(\tau)$ of the disc and its angular velocity

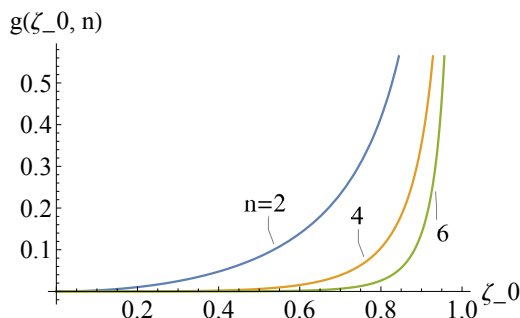


Figure 7: The functions $\langle g(\zeta_0, n) \rangle$ for $n = 2, 4, 6$, defined by (2.7).

$\omega(\tau)$ to provide a nonzero mean torque. The pseudo-scalar χ is nonzero for both cases (2.3) and (2.6 with n even) and provides the appropriate measure of chirality of the disc motion.

3. The two-sphere problem

Similar effects are to be expected for the two-sphere problem illustrated in Figure 1(a). Here we shall assume that the outer sphere S_2 with radius r_2 is fixed, and that the inner sphere S_1 with radius $r_1 < r_2$ oscillates on the line of centres so that the separation between the centres is

$$d(t) = d_0 + \zeta_0 \cos \tau \quad \text{with } 0 < d_0 \pm \zeta_0 < r_2 - r_1 \quad \text{and } \tau = \sigma t, \quad (3.1)$$

and simultaneously about the line of centres with time-periodic angular velocity $\omega(\tau)$, with period 2π and $\langle \omega(\tau) \rangle = 0$. The dotted spheres in Figure 1(a) indicate the range of the up-down oscillation. We further assume that suitably defined Reynolds and Stokes numbers are small, so that the flow, governed by the Stokes equations, is quasi-static and instantaneously determined by the no-slip boundary conditions. To this extent, the formulation is very similar to that of §2.

Following Jeffery(1912, 1915) and Papavasiliou & Alexander (2017), we adopt bi-spherical polar coordinates (ξ, φ, η) defined in terms of cylindrical polar coordinates (r, φ, z) by

$$\xi + i\eta = \log \left[\frac{r + i(z + R)}{r + i(z - R)} \right] \quad \text{or equivalently} \quad r + iz = R \frac{\sin \eta + i \sinh \xi}{\cosh \xi - \cos \eta}, \quad (3.2)$$

where R is an arbitrary positive real number. The contours $\xi = \text{const.}$ (solid) and $\eta = \text{const.}$ (dashed) are shown in Figure 8(a). From (3.2), it may be ascertained that

$$r^2 + (z - R \coth \xi)^2 = R^2 \text{cosech}^2 \xi. \quad (3.3)$$

Thus the contours $\xi = \text{const.}$ are circles with centres at $r = 0$, $z = R \coth \xi$, and radii $R \text{cosech} \xi$. For given (r_1, r_2, d) , it follows that ξ_1 , ξ_2 and R satisfy

$$R = r_1 \sinh \xi_1 = r_2 \sinh \xi_2, \quad (3.4)$$

and

$$r_1 \sinh \xi_1 - r_2 \sinh \xi_2 = 0, \quad r_1 \cosh \xi_1 - r_2 \cosh \xi_2 = -d. \quad (3.5)$$

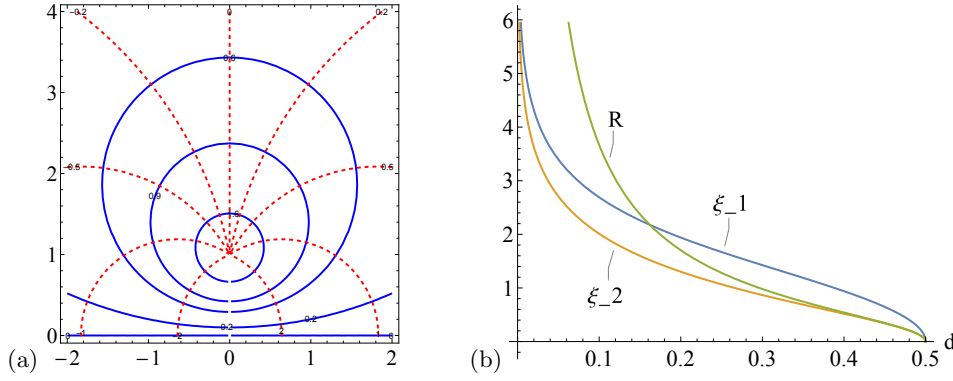


Figure 8: (a) Contours $\xi = \text{const.}$ (solid) and $\eta = \text{const.}$ (dashed) in the half-plane $z > 0$, as given by (3.2) for $R = 1$; (b) the functions $\xi_1(d)$, $\xi_2(d)$ (which tend logarithmically to infinity as $d \rightarrow 0$) and $R(d)$ for $r_1 = 0.5$, $r_2 = 1$, as given by (3.6) and (3.7).

These equations may be solved for $\cosh \xi_1$, $\cosh \xi_2$ and R^2 in terms of d , giving

$$\cosh \xi_1 = \frac{r_2^2 - r_1^2 - d^2}{2r_1 d}, \quad \cosh \xi_2 = \frac{r_2^2 - r_1^2 + d^2}{2r_2 d}, \quad (3.6)$$

and

$$R^2 = ((r_1 - r_2)^2 - d^2) ((r_1 + r_2)^2 - d^2) / 4d^2. \quad (3.7)$$

Note that d must be non-negative for real $\{\xi_1, \xi_2\}$. We may take $0 < d < r_2 - r_1$; these inequalities ensure that $\xi_1 > \xi_2 > 0$. Figure 1(a) actually shows the situation when $r_1 = 0.5$, $r_2 = 1$, $d = 0.25$ and $\zeta_0 = 0.2$, the dotted spheres indicating the limiting positions in the up-down oscillations. Fig 8(b) shows the functions $\xi_1(d)$ and $\xi_2(d)$ when $r_1 = 0.5$, $r_2 = 1$. More generally, $\xi_1(d)$ and $\xi_2(d)$ both vanish when $d = r_2 - r_1$, i.e. when the spheres are in contact. From (3.7), we then have asymptotically

$$r_1 \xi_1 \sim r_2 \xi_2 \quad \text{as } d \rightarrow r_2 - r_1. \quad (3.8)$$

In this contact limit, one might expect the torque to be dominated by local conditions near the contact point, but this is not in fact the case (see Appendix).

4. Transfer of angular momentum

In the Stokes approximation, with a purely azimuthal velocity field $\mathbf{u} = (0, v(r, z), 0)$, the pressure is constant throughout the fluid and

$$(\nabla^2 - r^{-2})v = 0. \quad (4.1)$$

The general solution of this equation in the above bi-spherical coordinates is:

$$v = \sqrt{W} \sum_{n=0}^{\infty} \{a_n \exp[(n + 1/2)(\xi - \xi_1)] + b_n \exp[-(n + 1/2)(\xi - \xi_2)]\} P_n^1(\cos \eta), \quad (4.2)$$

where $W \equiv R/(\cosh \xi - \cos \eta)$ (Jeffery 1915). The constants a_n and b_n are determined via the boundary conditions

$$v(\xi_1) = \omega(\tau) r_1, \quad v(\xi_2) = 0. \quad (4.3)$$

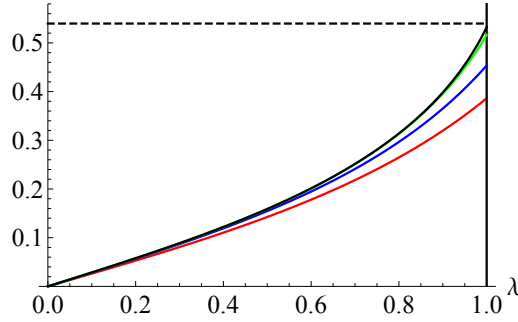


Figure 9: $\sum_{m=1}^n g_m(\lambda)$ for $r_1 = 0.5$, $d_0 = 0.25$ and for $n = 2$ (red), 3 (blue), 6 (green) and 10 (black); the sum to infinity is uniformly convergent, and in particular $\sum_{m=1}^{\infty} g_m(1) \approx 0.539667$.

The instantaneous torque $G(\tau)$ exerted on the outer sphere is then given by equation (11) from Jeffery (1915), which may here be expressed in the form

$$G(\tau) = 8\pi\mu r_1^3 \omega(\tau) \sum_{m=0}^{\infty} \frac{\sinh^3 \xi_1}{\sinh^3[(m+1)\xi_1(\tau) - m\xi_2(\tau)]}, \quad (4.4)$$

and the instantaneous torque experienced by the inner sphere is $-G(\tau)$. Since each term of the sum (4) is positive, it follows that $G(\tau)$ has the same sign as $\omega(\tau)$ at each instant τ , in accord with physical intuition[†].

We are again concerned with the mean torque exerted on the outer sphere,

$$\langle G \rangle = 8\pi\mu r_1^3 \sum_{m=0}^{\infty} \left\langle \frac{\omega(\tau) \sinh^3 \xi_1}{\sinh^3[(m+1)\xi_1(\tau) - m\xi_2(\tau)]} \right\rangle. \quad (4.5)$$

If we define $\lambda = \zeta_0/d_0$ and take $\omega(\tau) = \omega_0 \cos(\tau + \psi)$, this becomes

$$\langle G \rangle(r_1, d_0, \lambda) = 4\mu r_1^3 \omega_0 \cos \psi \sum_{m=0}^{\infty} g_m(r_1, d_0, \lambda), \quad (4.6)$$

where

$$g_m(r_1, d_0, \lambda) = \int_{\Delta} \frac{\cos \tau \sinh^3 \xi_1(\tau)}{\sinh^3[(m+1)\xi_1(\tau) - m\xi_2(\tau)]} d\tau, \quad (4.7)$$

and Δ is any 2π -period of τ , and $\xi_1(\tau)$ and $\xi_2(\tau)$ are given by (3.6) with now $d(t) = d_0(1 + \lambda \cos \tau)$. Figure 9 shows the functions $\sum_{m=1}^n g_m(r_1, d_0, \lambda)$ ($n = 2, 3, 6, 10$) with (by way of illustration) $r_1 = 0.5$, $d_0 = 0.25$, and for the relevant range of λ , i.e. $0 < \lambda < 1$. The sum (4.6) is uniformly convergent, even at the limiting value $\lambda = 1$ for which the spheres make contact and for which $\sum_{m=1}^{\infty} g_m(1) \approx 0.539667$.

The situation here is to be contrasted with that of Figure 4 which showed a divergent torque when the amplitude of the oscillation was maximal. In the present spherical case, the influence of the inner sphere on the outer sphere is much weaker in the contact limit, so weak in fact that the resulting torque is finite in this limit.

[†] Jeffery's expression for his G_1 is actually the torque exerted by the sphere S_1 on the fluid, and not as he states the torque experienced by S_1 . Of course, in our time-dependent situation, a torque $+G(\tau)$ would have to be exerted on the sphere S_1 by some internal battery mechanism to maintain its postulated rotational motion. An internal battery would also be needed to maintain the periodic up-down motion.

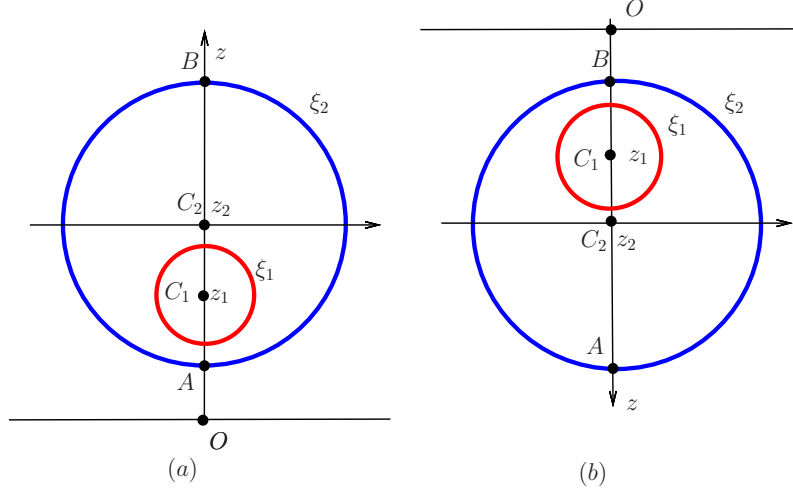


Figure 10: Reversal of z -coordinate if C_1 passes through C_2 ; (a) C_1 below C_2 ; (b) C_1 above C_2 .

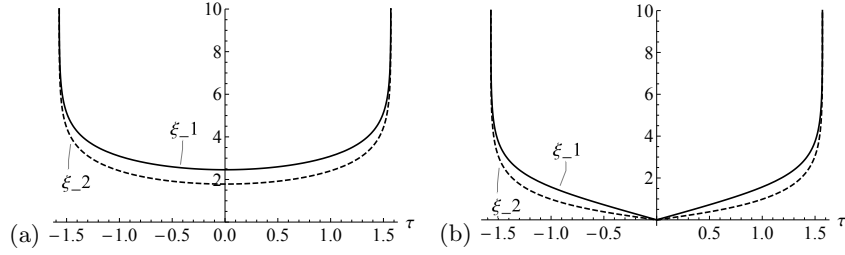


Figure 11: $\xi_1(\tau)$ and $\xi_2(\tau)$ in the time interval $-\pi/2 < \tau < \pi/2$ for (a) $\zeta_0 = 1/8$, (b) $\zeta_0 = 1/2$.

5. Oscillations symmetric about the centre of S_2

The above treatment requires minor modification if $d(\tau)$ is such that the centre C_1 of S_1 rises above the centre C_2 of S_2 in the course of its oscillations. As already indicated, ξ_1 and ξ_2 , as defined by (3.6) are real only if $d(\tau) > 0$ for all τ , i.e. only if C_1 remains below C_2 . If C_1 rises above C_2 , it is necessary to ‘switch’ the coordinate system by simply replacing z by $-z$ in (3.2); the situation is as represented in the sketch of Figure 10. This artifice ensures that $d(\tau) = z_2(\tau) - z_1(\tau)$ is indeed always positive.

Suppose for example that $d(\tau)$ is initially specified as $d(\tau) = \zeta_0 \cos \tau$, where the amplitude ζ_0 satisfies $0 < \zeta_0 < r_2 - r_1$. This may be used only when $d(\tau) > 0$, for example in the time interval $-\pi/2 < \tau < \pi/2$. Figure 11 shows $\xi_1(\tau)$ and $\xi_2(\tau)$ in this interval for the particular choices $\zeta_0 = 1/8$ and $\zeta_0 = 1/2$; the latter choice is maximal – for this value, the two spheres touch at time $\tau = 0$. Now if $\omega = \omega_0 \cos n\tau$, then just as in §2, the mean torque $\langle G \rangle$ on the sphere S_2 is zero or non-zero according as n is odd or even. Moreover, in the latter case, symmetry (in the mean) about the horizontal plane through C_2 allows us to calculate $\langle G \rangle$ by simply averaging over the π -interval $-\pi/2 < \tau < \pi/2$ (since the mean torque over the subsequent π -interval $\pi/2 < \tau < 3\pi/2$ will obviously be

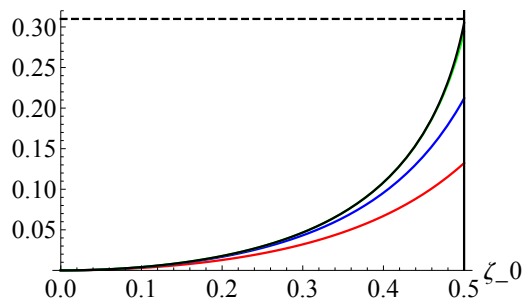


Figure 12: The torque $\langle G \rangle(\zeta_0)/4\mu r_1^3 \omega_0$ given by (5.1) and (5.2) for $r_1 = 1/2$ and $\omega = \omega_0 \cos 2\tau$; the partial sums $\sum_{m=1}^n h_m(\zeta_0)$ are shown for $n = 1$ (red), 2 (blue), 6 (green) and 10 (black); the sum converges to 0.3099 at $\zeta_0 = 1/2$ when the torque is maximal.

the same). Just as in (4.6), with $\omega = \omega_0 \cos 2\tau$ the mean torque is therefore given by

$$\langle G \rangle(r_1, \zeta_0) = 4\mu r_1^3 \omega_0 \sum_{m=0}^{\infty} h_m(r_1, \zeta_0), \quad (5.1)$$

where now

$$h_m(r_1, \zeta_0) = \int_{-\pi/2}^{\pi/2} \frac{\cos 2\tau \sinh^3 \xi_1(\tau)}{\sinh^3[(m+1)\xi_1(\tau) - m\xi_2(\tau)]} d\tau. \quad (5.2)$$

Figure 12 (which may be compared with Figure 9) shows the partial sums $\sum_{m=1}^n h_m(\zeta_0)$ for $n = 1$ (red), 2 (blue), 6 (green) and 10 (black). The convergence is obviously uniform and rapid. The sum converges to 0.3099 at $\zeta_0 = 1/2$ when the torque is maximal. Again the contrast between Figure 9 and Figure 7 which showed a divergent torque should be noted. For the spherical geometry, the interaction between the spheres is again so weak in the contact limit that the transmitted torque remains finite in this limit.

The above technique may be easily adapted to cover the more general case when $0 \leq d_0 < \frac{1}{2}(r_2 - r_1)$, $d_0 < \zeta_0 < r_2 - r_1 - d_0$, when the amplitude of the oscillations is large enough for C_1 to rise above C_2 but still small enough for S_1 to remain inside S_2 throughout the period of the oscillation. We need not labour the details here.

6. Conclusions and discussion

For the cartesian geometry of Figure 1(b), we have shown by straightforward analysis that time-periodic axisymmetric motion of the disc with zero mean can generate a mean torque on the two fixed plates bounding the fluid domain; in this, we have assumed quasi-static Stokes flow in which all inertia effects are negligible. Mean torque generation requires that the disc motion should have a chiral character, as measured by the pseudo-scalar quantity $\chi = \langle \omega(\tau)D(\tau) \rangle$, where $D(\tau) = (1 - d(\tau)^2)^{-1}$, and also that there should be a phase shift between its vertical and rotational components. In these respects, the generation of a mean torque is analogous to the dynamo generation of a mean (large-scale) magnetic field by a random-wave turbulence that is chiral and for which a phase shift is generated between the velocity and the resulting magnetic perturbation.

For the spherical geometry of Figure 1(a), we have demonstrated a similar phenomenon when the outer sphere S_2 is fixed and the inner sphere S_1 is subject to a time-periodic motion with zero mean velocity. We have given a clear physical interpretation of the

effect, namely that when S_1 is near to S_2 the rotational torque transmitted to S_2 is stronger than when it is far from S_2 . The phase shift is required, because without it the disc motion is time-reversible, and the reversibility theorem for Stokes flow ensures that, although the disc motion is still chiral, the instantaneous torque generated necessarily averages to zero. The spherical problem is significantly different from the planar problem in that the mean torque transmitted remains finite even in the limit when the spheres make instantaneous contact during a period of the up-down oscillation.

Although the analysis of the paper is restricted to Stokes flow, there seems little doubt that the effect must persist when fluid inertia is taken into account, because the above physical explanation is still applicable. It would be reasonably straightforward to take account of increasing frequency of the disc motion (i.e. increase of Stokes number), because the problem then remains linear. It would be much more difficult to take account of increasing Reynolds number, because there is then a nonlinear interaction between the poloidal and toroidal ingredients of the flow. Again, the problem has some similarity with the dynamo problem, in that explicit calculation of the α -effect in dynamo theory is easy only when the magnetic Reynolds number Re_m based on the random-wave scale is small, and very difficult when $Re_m \gg 1$ (Moffatt & Dormy 2019).

There is moreover no need to restrict the boundaries S_1 and S_2 to be spherical; the effect of chiral transfer will still obviously occur under similar circumstances if they are axisymmetric with a common axis of symmetry; and indeed the general principle of chiral transfer of angular momentum may be expected to have wide generality.

Appendix. Comment on the contact limit

We comment here on the inapplicability of conventional lubrication theory when the minimum gap between the two spheres tends to zero. It is sufficient to consider just the situation when $r_2 \rightarrow \infty$ so that S_2 becomes the plane boundary $z = 0$, and when the sphere S_1 makes contact with this plane; the situation is shown in Figure 13. If in this situation S_1 rotates about the diameter through the point of contact with *steady* angular velocity ω_0 , then, as observed by Papavasiliou & Alexander (2017), the torque G given by (4) reduces to

$$G \sim G_0 = -8\pi \mu r_1^3 \omega_0 \zeta(3), \quad (\text{A } 1)$$

where $\zeta(s) = \sum_{n=1}^{\infty} n^{-s}$ is the Riemann zeta function. When the sphere S_1 is remote from the plane, the well-known expression for the torque is

$$G \sim G_\infty = -8\pi \mu r_1^3 \omega_0, \quad (\text{A } 2)$$

so that

$$G_0/G_\infty = \zeta(3) \approx 1.20205. \quad (\text{A } 3)$$

Jeffery (1915) actually tabulated the value of the torque for various values of the ratio of the radius r_1 to the distance $r_1 + \epsilon$ where ϵ is the minimum gap between the sphere and the plane, and noted that, if $\epsilon/r_1 = 0.02$, “the couple required to maintain the rotation is only increased [from G_∞] by 17%”. We see from the above that in the contact limit $\epsilon = 0$, the couple is increased by only 20.2%.

Conventional lubrication theory (Batchelor 1967), would approximate the sphere $z/r_1 = 1 - (1 - (r/r_1)^2)^{1/2}$ near the point of contact by the paraboloid

$$z/r_1 = h(r) = \frac{1}{2}(r/r_1)^2, \quad (\text{A } 4)$$

shown in red in Figure 13. Lubrication theory is justifiable only in the ‘contact region’

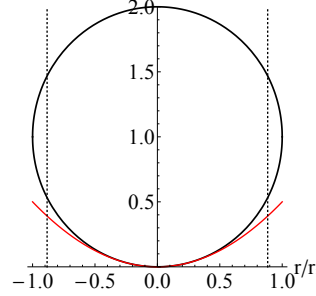


Figure 13: The limit when the sphere S_1 touches the plane $z = 0$; the sphere may be approximated near $r = 0$ by the paraboloid as shown in red, but the dominant contribution to the total torque comes from the region indicated by the dotted lines where lubrication theory is not applicable.

$r \ll r_1$. In this small region, the velocity profile is linear, i.e. locally Couette, and the contribution to the torque on S_1 out to radius r in this region is easily calculated as

$$G(r) \sim -2\pi \mu \omega_0 \int_0^r \frac{r'^3}{h(r')} dr' = -2\pi \mu r_1 \omega_0 r^2. \quad (\text{A } 5)$$

This increase with r resulting from the factor r'^3 in the integrand, indicates that the dominant contribution to the total torque in fact comes from outside this contact region, i.e. from the region $r = O(r_1)$ indicated by the dotted lines in Figure 13; there can be no justification for use of the lubrication approximation throughout this extended region.

We acknowledge helpful discussion with Prof. Gareth Alexander, University of Warwick. This research is partially supported by grant IG/SCI/ DOMS/18/16 from the Sultan Qaboos University, Oman.

REFERENCES

- BATCHELOR, G.K 1967 *An Introduction to Fluid Dynamics*, CUP.
- GRADSHTEYN, I. & RYZHIK, I. 2007 *Table of Integrals, Series, and Products*, Elsevier/Academic Press, Amsterdam, 7th ed.
- JEFFERY, G.B. 1915 On the steady rotation of a solid of revolution in a viscous fluid. *Proc. Lond. Math. Soc.* **2**, (1), 327-338.
- JEFFERY, G.B. 1912 On a form of the solution of Laplace's equation suitable for problem relating to two spheres. *Proc. R. Soc. Lond. A* **87**, 109-120.
- MOFFATT, H.K. 1978 *Magnetic Field Generation in Electrically Conducting Fluids.*, CUP.
- MOFFATT, H.K. & DORMY, E. 2019 *Self-Exciting Fluid Dynamos*, CUP (publication imminent).
- PAPAVASILIOU, D. & ALEXANDER, G.P. 2017 Exact solutions for hydrodynamic interactions of two squirming spheres. *J. Fluid Mech.* **813**, 618-646.